23. Agarwal A, Garg A (2010) Enzymatic activity of the human 1-acylglycerol-3-phosphate-O-acyltransferase isoform 11: upregulated in breast and cervical cancers. J Lipid Res 51: 2143–2152.
24. Falvella FS, Pascale RM, Gariboldi M, Manenti G, De Miglio MR, et al. (2002) Stearoyl-CoA desaturase 1 (Scd1) gene overexpression is associated with genetic predisposition to hepatocarcinogenesis in mice and rats. Carcinogenesis 23: 1933–1936.
25. Scaglia N, Igal RA (2008) Inhibition of Stearoyl-CoA Desaturase 1 expression in human lung adenocarcinoma cells impairs tumorigenesis. International journal of oncology 33: 839–850.
26. Linkous A, Yazlovitskaya E (2010) Cytosolic phospholipase A2 as a mediator of disease pathogenesis. Cell Microbiol.
27. Shindou H, Hishikawa D, Harayama T, Yuki K, Shimizu T (2009) Recent progress on acyl CoA: lysophospholipid acyltransferase research. J Lipid Res 50 Suppl: S46–51.
28. Cazares LH, Troyer DA, Wang B, Drake RR, John Semmes O (2011) MALDI tissue imaging: from biomarker discovery to clinical applications. Anal Bioanal Chem 401: 17–27.
29. Schwamborn K, Krieg RC, Reska M, Jakse G, Knuechel R, et al. (2007) Identifying prostate carcinoma by MALDI-Imaging. Int J Mol Med 20: 155–159.
30. Rauser S, Marquardt C, Balluff B, Deininger SO, Albers C, et al. (2010) Classification of HER2 receptor status in breast cancer tissues by MALDI imaging mass spectrometry. J Proteome Res 9: 1854–1863.
31. Thiery G, Shchepinov MS, Southern EM, Audebourg A, Audard V, et al. (2007) Multiplex target protein imaging in tissue sections by mass spectrometry–TAMSIM. Rapid Commun Mass Spectrom 21: 823–829.

Identification of oligosaccharides from histopathological sections by MALDI imaging mass spectrometry

Masanori Yamada, Ikuko Yao, Takahiro Hayasaka, Masaru Ushijima, Masaaki Matsuura, Hideho Takada, Nobuaki Shikata, Mitsutoshi Setou, et al.

Analytical and Bioanalytical Chemistry

ISSN 1618-2642

Anal Bioanal Chem
DOI 10.1007/s00216-011-5622-y

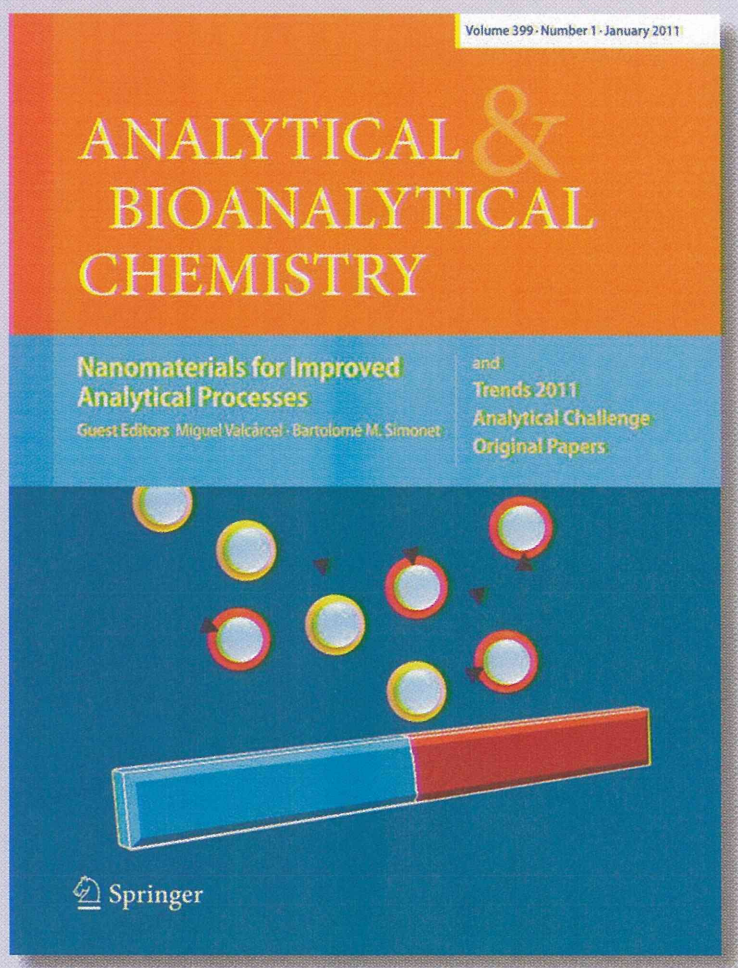

Springer

Anal Bioanal Chem
DOI 10.1007/s00216-011-5622-y

ORIGINAL PAPER

Identification of oligosaccharides from histopathological sections by MALDI imaging mass spectrometry

Masanori Yamada · Ikuko Yao · Takahiro Hayasaka · Masaru Ushijima · Masaaki Matsuura · Hideho Takada · Nobuaki Shikata · Mitsutoshi Setou · A-Hon Kwon · Seiji Ito

Received: 28 September 2011 / Revised: 28 November 2011 / Accepted: 28 November 2011

Abstract Direct tissue analysis using matrix-assisted laser desorption/ionization (MALDI) mass spectrometry (MS) provides the means for in situ molecular analysis of a wide variety of biomolecules. This technology—known as imaging mass spectrometry (IMS)—allows the measurement of biomolecules in their native biological environments without the need for target-specific reagents such as antibodies. In this study, we applied the IMS technique to formalin-fixed paraffin-embedded samples to identify a substance(s) responsible for the intestinal obstruction caused by an unidentified foreign body. In advance of IMS analysis, some pretreatments were applied. After the deparaffinization of sections, samples were subjected to enzyme digestion. The sections co-crystallized with matrix were desorbed and ionized by a laser pulse with scanning. A combination of α-amylase digestion and the 2,5-dihydroxybenzoic acid matrix gave the best mass spectrum. With the IMS Convolution software which we developed, we could automatically extract meaningful signals from the IMS datasets. The representative peak values were *m/z* 1,013, 1,175, 1,337, 1,499, 1,661, 1,823, and 1,985. Thus, it was revealed that the material was polymer with a 162-Da unit size, calculated from the even intervals. In comparison with the mass spectra of the histopathological specimen and authentic materials, the main component coincided with amylopectin rather than amylose. Tandem MS analysis proved that the main components were oligosaccharides. Finally, we confirmed the identification of amylopectin by staining with periodic acid-Schiff and iodine. These results for the first time show the advantages of MALDI-IMS in combination with enzyme digestion for the direct analysis of oligosaccharides as a major component of histopathological samples.

M. Yamada · H. Takada · A.-H. Kwon
Department of Surgery, Kansai Medical University,
2-3-1 Shin-machi,
Hirakata, Osaka 573-1191, Japan

I. Yao · S. Ito
Department of Medical Chemistry, Kansai Medical University,
10-15 Fumizono-cho,
Moriguchi, Osaka 570-8506, Japan

I. Yao (✉)
Precursory Research for Embryonic Science and Technology
(PRESTO), Japan Science and Technology Agency (JST),
7 Goban-cho,
Chiyoda-ku, Tokyo 102-0076, Japan
e-mail: yaoik@takii.kmu.ac.jp

T. Hayasaka · M. Setou
Department of Molecular Anatomy,
Hamamatsu University School of Medicine,
1-20-1 Handayama, Higashi-ku,
Hamamatsu, Shizuoka 431-3192, Japan

M. Ushijima · M. Matsuura
Bioinformatics Group, Genome Center,
Japanese Foundation for Cancer Research,
3-8-31 Ariake,
Koto-ku, Tokyo 135-8550, Japan

M. Matsuura
Division of Cancer Genomics, Cancer Institute,
Japanese Foundation for Cancer Research,
3-8-31 Ariake,
Koto-ku, Tokyo 135-8550, Japan

N. Shikata
Department of Clinical Sciences and Laboratory Medicine,
Kansai Medical University,
10-15 Fumizono-cho,
Moriguchi, Osaka 570-8506, Japan

Published online: 13 December 2011

Keywords Imaging mass spectrometry · MALDI-TOF MS · Bioanalytical methods · Amylase · Amylopectin · Oligosaccharide

Abbreviations

DHB	2,5-Dihydroxybenzoic acid
FFPE	Formalin-fixed paraffin-embedded
HE	Hematoxylin and eosin
IMS	Imaging mass spectrometry
ITO	Indium tin oxide
MALDI	Matrix-assisted laser desorption/ionization
PAS	Periodic acid-Schiff stain
ROI	Region of interest
CT	Computed tomography

Introduction

Recently, imaging mass spectrometry (IMS) has emerged and was dramatically developed for proteomic and metabolomic analyses [1, 2] in many fields including biology [3, 4] and pathology [5, 6]. Direct tissue analysis using matrix-assisted laser desorption/ionization (MALDI)-MS provides the means for the in situ molecular analysis of a wide variety of biological molecules. In IMS, the mass spectra associated with spatial information can be continuously recorded to obtain the expression patterns of various molecules in the specimens to be analyzed [7–11]. With this technique, we can perform MS directly from tissue sections and analyze biological compounds [12–14]. This technology allows the measurement of these species without the need for target-specific reagents such as antibodies [15, 16]. MALDI-IMS enables us to obtain the molecular constituents of the object substance along with local information of various unknown components in a single measurement. In recent years, a great many advances in the practice of IMS have occurred, making the technique more sensitive and useful [17]. A major advantage of direct MALDI analysis is that it avoids time-consuming extraction, purification, or separation steps, which have the potential of producing artifacts. One of the recent applications of MALDI MS is its use to profile and image components directly from tissue sections [7, 18].

We and other groups have proposed methods for performing in situ proteomic analyses by IMS as an additional efficient technique for proteomic analysis to two-dimensional electrophoresis [1, 15, 16]. Moreover, IMS procedure has begun to be used for formalin-fixed paraffin-embedded (FFPE) samples that are commonly used in hospitals and stored for a long time [19]. Here, we applied the IMS technique for FFPE histological analyses of the substance of intestinal obstruction material.

Bowel obstruction or intestinal obstruction is a mechanical or functional obstruction of the intestine that prevents the normal transit of digested materials. It can occur at any levels distal to the duodenum of the small intestine and is typically considered to represent a medical emergency. For the case in this study, surgery was needed to remove the necrotic tissue and causative materials. Even after the materials were removed, the cause and the identity of the materials were not clarified. To obtain information of the extirpated materials, the IMS technique was employed.

Methods

Materials

Human sample analysis in this study was started after approval of the ethical committee of Kansai Medical University and followed the committee's requests regarding informed consent.

α-Amylase (A0521, 1,000–1,500 U/mg, lyophilized powder, derived from human saliva) was purchased from Sigma-Aldrich (St. Louis, MO, USA). Calibration standard peptides and 2,5-dihydroxybenzoic acid (DHB) were purchased from Bruker Daltonics (Leipzig, Germany). Iodine and potassium iodide were obtained from Yoshida Pharmaceutical Co. Ltd. (Tokyo, Japan) and Merck (Darmstadt, Germany), respectively. The traditional rice cake known as *mochi* in Japan, which is made from glutinous rice, was purchased from a local market. Starches made from rice, potato, wheat, and corn were also obtained in the local market. High-amylose starch was obtained from Nihon Shokuhin Kako Co. Ltd. (Tokyo, Japan).

Diagnosis, examinations, and operations of intestinal obstruction

In the physical examination, localized tenderness was identified in the umbilical region. After computed tomography (CT) scanning, the pain had progressed severely and there was rebound tenderness and muscle guarding in the same area. Contrast-enhanced CT showed the high-density mass in the dilated small intestine and air fluid level formation in the right iliac fossa. Laparoscopic operation was performed to excise the inflamed small intestine and the obstructive material. The laparoscopy-assisted operation was performed with a three-port system. Serous and yellow ascites were present in the right iliac fossa and not inflamed in the appendix, gallbladder, ovaries, and other organs in the abdominal cavity. A foreign body was detected in the dilated and inflamed ileum at 100 cm from the ileum end. That small intestine was resected with assisted laparoscopy. The surgically isolated intestinal portion and the foreign body

were fixed and paraffin-embedded as performed routinely at Kansai Medical University Hospital and then subjected to IMS analysis.

Sample preparation with on-tissue digestion

The samples in paraffin blocks were cut into 4-μm sections and mounted onto an indium tin oxide (ITO)-coated glass slide (Bruker Daltonics). Paraffin was removed with xylene from the sample to give the enzyme complete access to the sample followed by crystallization with matrix. In detail, before clearing, the samples were heated to melt the paraffin and then washed multiple times with xylene to remove the paraffin. Xylene was removed and the sample was rehydrated by graded washes with xylene and ethanol, and then through graded washes of ethanol in water, ending in a final rinse in pure water. Deparaffinized sections on an ITO-coated glass slide were subjected to a small amount of enzyme digestion using 10 U/mL of α-amylase in 0.1 M phosphate buffer (pH 6.4) at 37 °C for 2 h in a humidified chamber so as not to disrupt the configuration of the components in the sample. Glass slides were dried using a SpeedVac vacuum at room temperature. The matrix solution containing 50 mg/mL of DHB in 70% methanol and 0.1% trifluoroacetic acid was uniformly sprayed over the samples using a 0.2-mm nozzle caliber airbrush (Procon Boy FWA Platinum, Mr. Hobby, Tokyo, Japan), and the same solution was dropped onto a portion of the section. The samples were subjected to laser scanning for MALDI-IMS or tandem mass spectrometry (MS/MS).

As a reference, a small portion of *mochi* (about 5×5×10 mm) or boiled dumplings containing high-amylose starch was fixed with 4% paraformaldehyde and treated according to the same procedure used to prepare the histopathological sample. The *mochi* and dumpling samples were then subjected to direct MALDI-MS analyses.

Imaging mass spectrometry

We adopted the procedures for MALDI-IMS described previously [6, 12], with some modifications. After applying the coating matrix, the histopathological sections were analyzed using a MALDI-TOF/TOF-type instrument, Ultraflex II (Bruker Daltonics), which was equipped with a 355-nm Nd:YAG laser. A 200-Hz repetition rate was used. Data were acquired in the positive ion mode using an external calibration method. Calibration proteins were deposited on the surfaces of sample support materials to minimize mass shift. The interval between data points was 50 μm, and 100 shots of laser beam were irradiated on each data point. The IMS dataset acquired by a Mass Microscope (Shimadzu, Kyoto, Japan) was converted to analyze the format file to enable analysis with the BioMap free software and the IMS Convolution software, which we have developed, as well as Bruker's software.

Data analysis

To extract the *m/z* values of the major peaks, we used our custom-designed IMS Convolution software with the common peak method [20]. For peak detection, we set a *k*-nearest neighborhood as a width of window on the *x*-axis (or *m/z*-axis); an *m/z* value achieving the maximum intensity in each window is regarded as a peak. The window is moved along the *x*-axis and the peaks are searched in the mass spectrum of each measurement point. Moreover, we set two regions of interest (ROIs) on the histopathological sample and outside using an optical image corresponding to the entire measurement area. The optical image was automatically extracted using a Mass Microscope. The IMS Information software, which is also custom-designed, is produced by Shimadzu Co. The settings of window size and the divided number are optimized to automatically set ROIs on an optical image. The area information output is provided as a text format and loaded into IMS Convolution. The common peaks are searched within each area. Common peaks are defined by the point x in which an average of peaks, $A(x)$, is greater than a certain threshold, h. Here, the $A(x)$ of ROI r, say $A_r(x)$, was calculated by averaging Gaussian kernels with center at the individual peak, as expressed follows:

$$A_r(x) = \frac{1}{N_r} \sum_{i=1}^{N_r} \sum \exp\left[-\frac{(x - p_{i,j})^2}{(\sigma p_{i,j})^2} \right].$$

where N_r is the number of data points in ROI r, $p_{i,j}$ is the *m/z* value of the ith subject's jth peak, and σ is a parameter accounting for the width of the peak. The common peaks are listed on each area in the csv format file and used to reconstruct the ion images using BioMap. The maximum values to reconstruct ion images were optimized to be clear.

Image reconstruction

Image reconstruction from signals in the spectra was performed using FlexImaging (Bruker Daltonics) as previously described [12]. Because the ionization efficiency could vary depending on the matrix–analyte co-crystallization conditions and their sublimation during measurement [12, 15], the absolute intensities of the mass spectra were normalized to the same value of total ion current to eliminate the variations of ionization efficiency. After the normalization process, ion images were reconstructed from signals in the spectra using FlexImaging.

MS/MS analyses

Tandem mass spectrometry analysis was performed using a Mass Microscope (Shimadzu). The Nd:YAG laser was run at 1,000 Hz and the mass spectra were mainly obtained from 200 laser shots per measurement point. In the MS/MS operation, the data acquisition conditions (i.e., the laser power, collision energy, and number of laser irradiations) were optimized in order to obtain product ion mass spectra with high signal-to-noise ratios (S/N) of the fragment peaks.

Special staining of paraffin section

The paraffin section samples were prepared and then deparaffinized sections were subjected to general or special histopathological staining. Hematoxylin–eosin (HE) staining, periodical acid-Schiff (PAS), PAS diastase (D-PAS) [21], Alcian blue, Kossa, Dylon, and Congo red staining were performed. S-100 protein detection, immunostaining with anti-S100 antibody, was performed. To detect human macrophages, CD68 immunostaining [22] was carried out. Silver impregnation was also conducted. These staining procedures were conducted according to established methods for histopathological examination at the Department of Clinical Sciences and Laboratory Medicine in Kansai Medical University. For the iodide reaction, 2% iodine and 4% potassium iodide solution was used at room temperature.

Results and discussion

Workflow of the sample preparation with enzyme digestion for IMS

For IMS analysis, the outline of the procedure for direct mass imaging in this study is shown in Fig. 1. The affected region of the small intestine and the foreign substances were removed with laparoscopic assistance (Fig. 1a). Surgically isolated intestine and the foreign body were fixed and paraffin-embedded as routinely performed at the Kansai Medical University Hospital. The histopathological sections were prepared from FFPE blocks of the removed intestine and the foreign body. Then, the 4-μm sections were extended on ITO-coated glass slides. Deparaffinized sections on ITO-coated glass slides were subjected to IMS analysis (Fig. 1b). First, we tried to obtain the mass spectra without any pretreatment; no signals were found. Since we did not have information about the constituents of the foreign body, we then tried to make

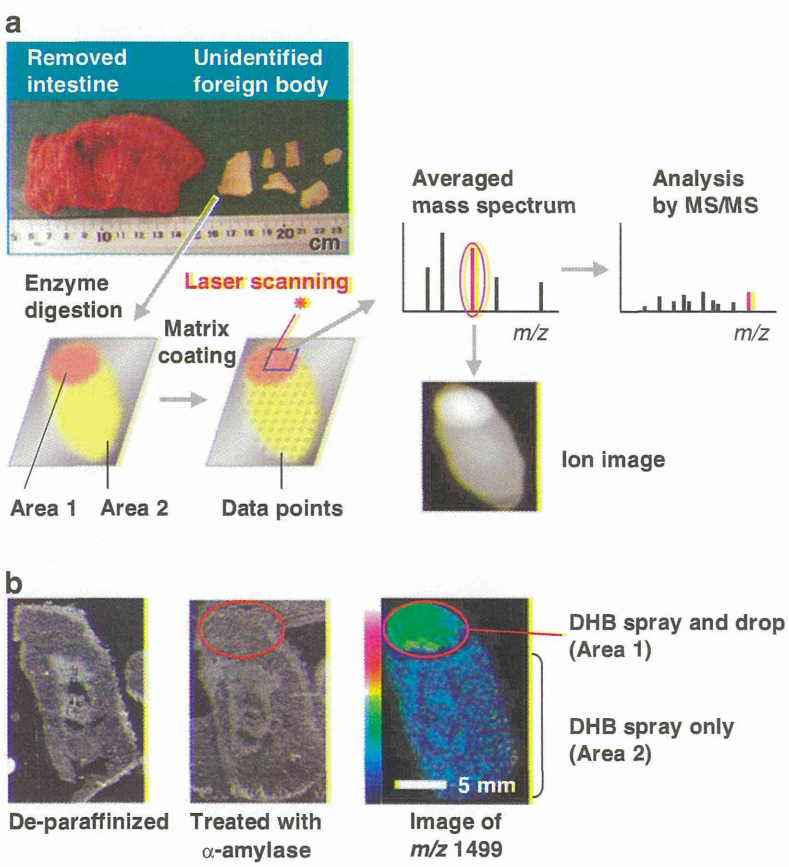

Fig. 1 Overview of the imaging mass spectrometry (IMS) procedure. **a** Appearance of the isolated portion of the surgically removed small intestine and the unidentified foreign body (*upper panel*) and the workflow of sample preparation for IMS. Samples in the paraffin blocks were sliced into 4-μm-thin sections, mounted on ITO-coated slide glasses, and then deparaffinized. After digestion with α-amylase, the samples were coated with DHB matrix by uniform spraying and addition of droplets. The well-dried samples on the slide were subjected to laser scanning for MALDI-IMS followed by ion image reconstruction. The spectra of particular interest (*red line*) were examined by tandem mass spectrometry. **b** Samples at three stages of the IMS procedure. The *red circle* designated as "*Area 1*" shows the region added with the DHB droplet. The other region is termed "*Area 2*"

fragmentation of the material with enzyme digestion (Fig. 1b). We applied amylase for carbohydrate- or oligosaccharide-like materials and trypsin for protein-like materials. Then, the matrix solution was sprayed on the section samples. For the samples that were not treated with α-amylase or without matrix addition, we hardly detected or did not obtain any signals upon laser exposure (data not shown). Because the spray droplet method [12] enhances the ionization efficiency for MALDI-IMS, a small amount of matrix solution was dropped onto the slide after the DHB spray (area 1, red circle in Fig. 1b). The slide was then dried and subjected to IMS analysis. In total, stronger signals were detected in area 1 than in area 2. For example, the signal intensity of the molecule represented by *m/z* 1499 was higher in area 1 (Fig. 1b); other molecules had high signal intensities in the area (Figs. 2 and 3). Thus, we mainly focused on area 1 for subsequent analyses.

Direct mass imaging analysis of the histopathological section

After data acquisition, the IMS dataset was converted to the ANALYZE 7.5 format file for loading to BioMap, as described previously [13], and to our custom-designed IMS Convolution software [23]. The peaks were extracted from the large IMS dataset manually with BioMap and automatic procedures with the IMS Convolution software, with information on ROIs such as areas 1 and 2. When the peaks were extracted manually from the averaged mass spectrum of all spots in area 1 from the BioMap peak pattern, the averaged mass spectra were provided as output in text format files and labeled one by one (Fig. 2a). To automatically extract the meaningful *m/z* values of the major peaks with ROI information from the IMS datasets, we applied the IMS Convolution software. The processing is based on the detection of "common peaks" [20] within the ROIs. With the IMS Convolution software, the peak values in areas 1 and 2 were automatically extracted and exported as a text file. The calculated values designated as common peaks were plotted in the graph, which reflected the frequency of appearance and the signal intensities (Fig. 2b).

The molecule represented by *m/z* 1,175 was detected with the highest intensity (Fig. 2a), and the molecule represented by *m/z* 1,337 was detected at the highest frequency (Fig. 2b). A few peaks were detected from area 2 (Fig. 2c). The spectral patterns shown in Fig. 2 suggest that the foreign body was composed of polymers. Moreover, the pitch width of each major peak was *m/z* 162 (Table 1). Other peaks were also observed, such as isotopic signals ([M+1] and [M+2], details not shown), sodium adduct ($[M + Na]^+$), and potassium adduct ($[M + K]^+$), judged from the differences of the *m/z* values from major peaks. The signal intensities of $[M + Na]^+$ were higher than $[M + K]^+$, mainly

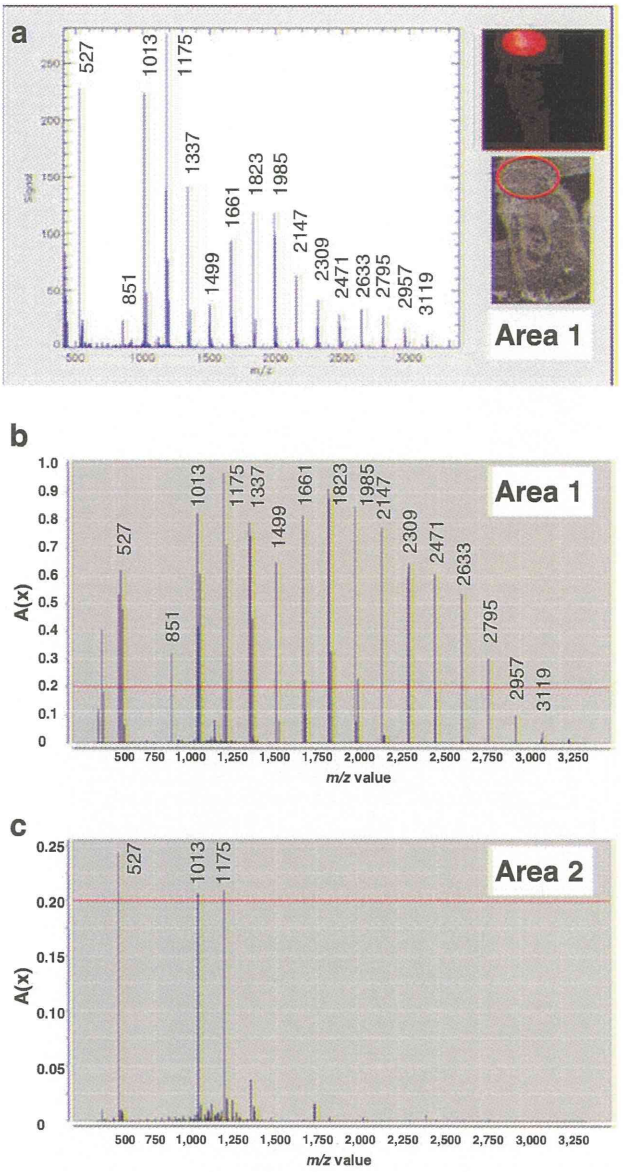

Fig. 2 Peaks obtained from the histopathological paraffin section by IMS. **a** Average of spectra of area 1 drawn using BioMap software. Major peaks were selected and the indicated *m/z* values were labeled manually. **b**, **c** Peaks of areas 1 and 2 extracted using the IMS Convolution software. The major peaks are extracted as common peaks and displayed as the spectra of $A(x)$. The threshold value is indicated by the *red lines* at 0.2

because sodium phosphate buffer was used for enzyme digestion.

Image reconstruction of the histopathological section

The distribution patterns of some ions which had *m/z* 162 intervals were reconstructed from the IMS data (Fig. 3). Those were picked up by the $A(x)$ value 0.2 as thresholds, except for large molecules at *m/z* 2,957 and at *m/z* 3,119.

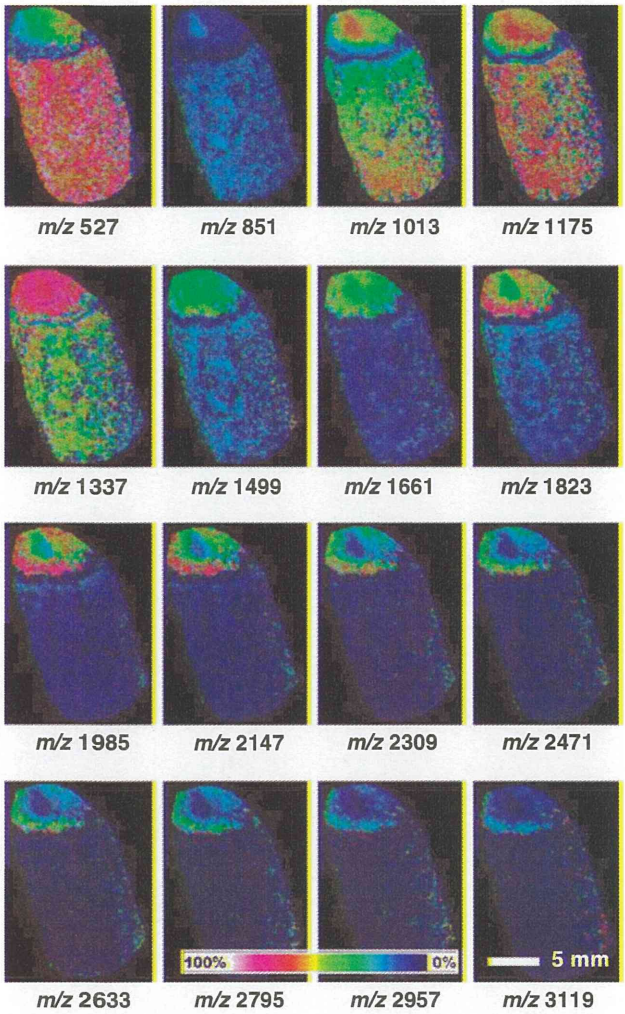

Fig. 3 Imaging mass spectrometry analyses of the histopathological paraffin section. Reconstructed images of the major peaks of area 1 extracted by the IMS Convolution software shown in Fig. 2b and Table 1. The signal intensity is shown in *pseudo-rainbow-colored images*

Reconstructed ion images in Fig. 3 show that the spray droplet method [12] was effective for ionization of a wide variety of *m/z* molecules, from *m/z* 527 to *m/z* 3,119, especially for the high *m/z* value region. The abundance of each molecule detected in areas 1 and 2 was not parallel. For example, ion at *m/z* 1,337 was most abundant in area 1, whereas ion at *m/z* 527 was the main signal in area 2. The results show that the efficiency of ionization could be changed by the *m/z* value, abundances of the analytes, and the ionization procedure of how to make an analyte–matrix complex.

Comparison with amylopectin and high-amylose starch

Because enzyme treatment gave good quality mass spectra, it was suggested that the component of the foreign body was oligosaccharide, the substrate of α-amylase. α-Amylase

Table 1 Extracted common peaks of areas 1 and 2

A(*x*)	Major peaks (*m/z*)	Peaks (*m/z*)	Interval of major peaks (*m/z*)	Differences between the head peaks (*m/z*)
0.53	527	527	104	
0.62		*543*		16
0.32	851	851	324	
0.82	1,013	1,013	162	
0.61		*1029*		16
0.97	1,175	1,175	162	
0.68		*1,191*		16
0.71	1,337	1,337	162	
0.44		*1,353*		16
0.65	1,499	1,499	162	
0.82	1,661	1,661	162	
0.24		*1,677*		16
0.82	1,823	1,823	162	
0.22		*1,840*		16
0.91	1,985	1,985	162	
0.79	2,147	2,147	162	
0.65	2,309	2,309	162	
0.54	2,471	2,472	162	
0.43	2,633	2,633	162	
0.30	2,795	2,795	162	
	2,957	2,957	162	
	3,119	3,119	162	
0.24	(Area 2)	527		
0.21	(Area 2)	1,013	486	
0.21	(Area 2)	1,175	162	

Values in italics are derived from $[M + K]^+$

(EC# 3.2.1.1) is an endo-type 1,4-α-D-glucan glucanohydrolase; maltose and polysaccharides with more than three residues of glucose are produced. A representative substrate of α-amylase, starch is classified into amylose and amylopectin. Natural starches are a mixture of amylose (10–20%) and amylopectin (80–90%). The traditional rice cake known as *mochi* in Japan, which is made from glutinous rice, is entirely composed of amylopectin.

We compared the spectral pattern of the histopathological section with those of an authentic *mochi* sample (no amylose and 100% amylopectin) and some kinds of starch containing various rates of amylose. Common rice starch contains 15–20%, potato starch and wheat starch have 20–25%, corn starch contains 25%, and high-amylose starch contains about 50% amylose. The reference materials were treated with the same procedures as the histopathological sample and analyzed with direct MALDI-MS analyses. The spectral patterns of starch containing amylose and *mochi* were different, and that of the histopathological sample coincided with the latter (Fig. 4). Both the histopathological

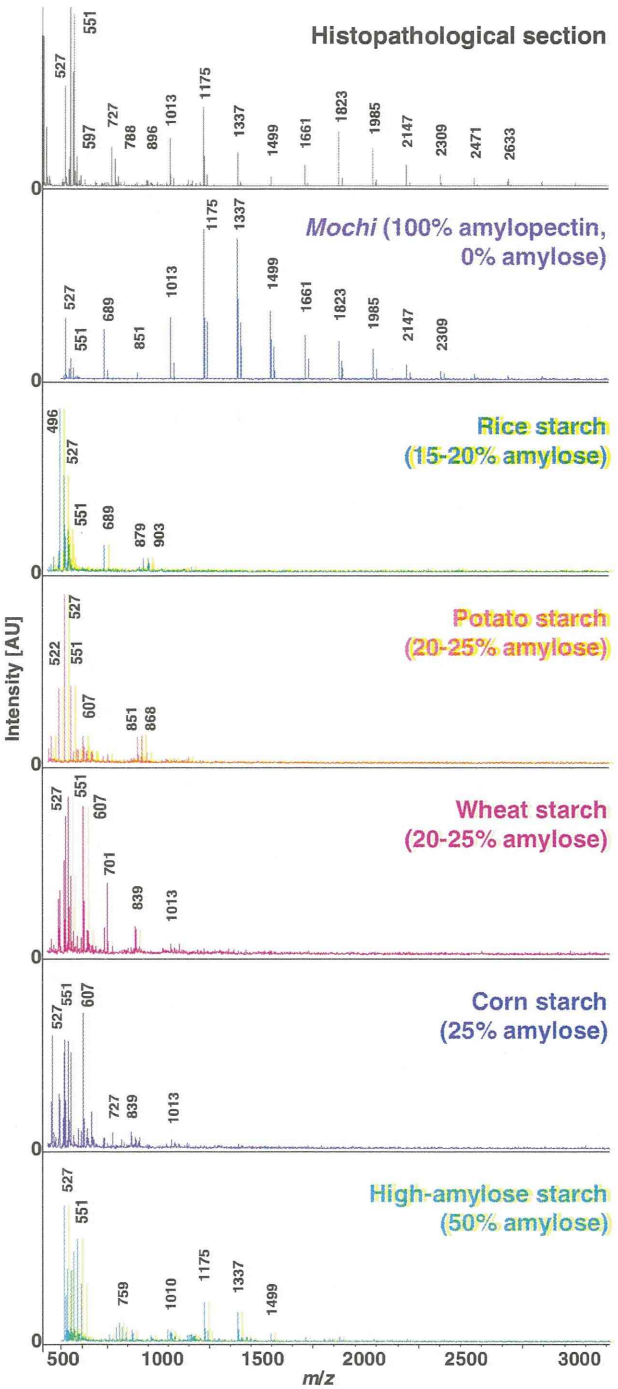

Fig. 4 Comparison of mass spectra with amylopectin and amylose. The mass spectra were obtained from the pathological section of the foreign body and authentic materials prepared from *mochi* and various kinds of starch. *Mochi* has no amylose, whereas other starches have different contents of amylose. All samples were subjected to α-amylase digestion and attached to the DHB matrix. Signals were obtained using UltraFlex II. Signal intensities in the graph were determined by relative intensity with arbitrary unit (*AU*)

sample and authentic *mochi* had polymer-like signals to the relatively large mass range, whereas other starches did not have such even interval signals (Fig. 4). This may be explained by the notion that amylopectin is difficult to be digested by α-amylase due to the α-(1-6)-D-glycopyranosyl branches. Other starches had signals with lower *m/z* regions, suggesting that the pretreatment with α-amylase digested extensively glucose linkages. These results provide strong evidence that the material causing the obstruction was *mochi*. Treatment with α-amylase produced many peaks at essentially equidistant intervals with an *m/z* value of 162. The maximum *m/z* value detected was 3,119, which

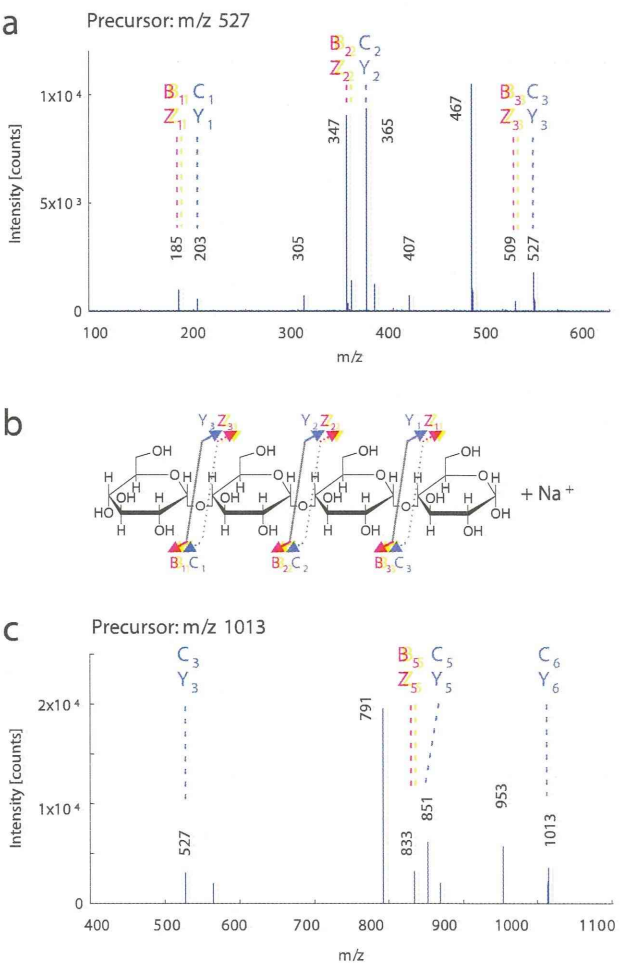

Fig. 5 Tandem mass spectrometry of polyglucose from the paraffin sections of the foreign body. **a** The ions of the diagnostic fragments suggest that the ions at *m/z* 527 are from polyglucose. Direct MS/MS spectrum of the precursor ion at *m/z* 527—fragmentations of the ions of 4-mer oligosaccharides. **b** Nomenclature of fragment ions and scheme of the observed glycosidic cleavages. **c** Direct MS/MS spectrum of the precursor ion at *m/z* 1,013—fragmentations of the ions of 6-mer oligosaccharides. Tandem mass spectrometry experiments were performed with a Mass Microscope. Signal intensities in the graph were determined by the MS count (**a**, **c**)